PIER C

(Received 17 April 2025, Accepted 8 July 2025, Scheduled 18 July 2025)

Compact Stepped-Impedance Low-Pass Filter Using Coplanar Open-Circuited Stubs

Yi-Ruo Chen, Kuan-Wei Chen*, and Chun-Long Wang

National Taiwan University of Science and Technology, Taipei 106335, Taiwan

ABSTRACT: This paper proposes a compact stepped-impedance low-pass filter using coplanar open-circuited stubs. The coplanar open-circuited stubs, which are used to compensate for the capacitive effect of the stepped-impedance low-pass filter, are implemented underneath the stepped-impedance low-pass filter. Consequently, the size of the stepped-impedance low-pass filter can be significantly reduced from 11.1 mm × 23.4 mm to 5.6 mm × 9.4 mm without altering its performance, amounting to a reduction rate of 79.83%. In addition, the transmission coefficient is attenuated below −30 dB, which is less than −20 dB attenuation of the conventional stepped-impedance low-pass filter. To verify the simulation result, the conventional stepped-impedance low-pass filter and the compact stepped-impedance low-pass filter using coplanar open-circuited stubs are fabricated and measured where the measurement results agree well with the simulation ones.

1. INTRODUCTION

In modern communication systems and electronic devices, microwave filters play a crucial role in signal selectivity, which can be accomplished by determining specific passbands and stopbands in the frequency response of the components. Among the microwave filters, low-pass filters are critical for the entire communication system, making them essential in many applications. Low-pass filters are widely used to filter out high-frequency noise and unwanted signals. However, low-pass filters may face size, cost, and power consumption limitations, making compact low-pass filters important for enhancing system performance and cost savings.

In the past, scholars have proposed different methods for out-of-band rejection and specification design for filters. Cohn introduced one of the earliest single-frequency bandpass filters using microstrip lines in 1958, known as parallel-coupled line bandpass filter [1]. Due to its simple structure and good response, it is frequently used in communication systems. However, parallel-coupled lines can generate high-frequency harmonics in the stopband due to the different phase velocities of odd and even modes at high frequencies. Many studies have since explored ways to suppress these harmonics [2–5]. Among them, stepped-impedance resonators [2] are commonly used in the low-pass filter design to suppress these harmonics. However, they face issues with large sizes and limitations in the stopband. As a result, another noted approach in low-pass filter design, which adopts 1 Defected Ground Structure (DGS) is proposed [6–9]. DGS is implemented by etching slots in the ground plane, where the disrupted current distribution in the etched areas exhibits resonant characteristics to suppress spurious responses in the stopband. However, due to the disruption of the ground plane current, DGSs can introduce non-ideal effects at high frequencies, degrading the signal quality.

Another commonly used filter structure is hairpin filter [10–13]. Hairpin filter has a simple structure, typically consisting of two or more parallel resonant cavities and coupled hairpin structures. In addition to being easy to implement, hairpin filters generally offer higher filtering performance than conventional stepped-impedance filters, achieving deep stopband attenuation. However, hairpin filters usually have a large size and require considerable coupling calculations, making their design process complex.

As a result, the stepped-impedance low-pass filter is chosen as the prototype of the low-pass filter design. However, since the stepped-impedance low-pass filter suffers from the disadvantage of large size, coplanar open-circuited stubs are used to miniaturize the size of the stepped-impedance low-pass filter without degrading the performance of the filter. The details of the paper are described below. Section 1 introduces the literature survey of the filters. Section 2 describes the conventional stepped-impedance low-pass filter. Section 3 addresses the details of the compact stepped-impedance low-pass filter using coplanar open-circuited stubs. Section 4 concludes this paper.

2. CONVENTIONAL STEPPED-IMPEDANCE LOW-PASS FILTER

The schematic view of the conventional stepped-impedance low-pass filter is shown in Fig. 1 where the substrate used is FR4 with a relative dielectric constant of $\epsilon_r = 4.4$, a loss tangent of $\tan\delta = 0.02$, and a thickness of $h = 1.6$ mm. Given the specifications of the filter: the −3-dB cutoff frequency of 2.5 GHz, the 5-GHz attenuation of −20 dB, and the characteristic impedance of 50 Ω, the dimensions of the con-

* Corresponding author: Kuan-Wei Chen (ethan041891@gmail.com).

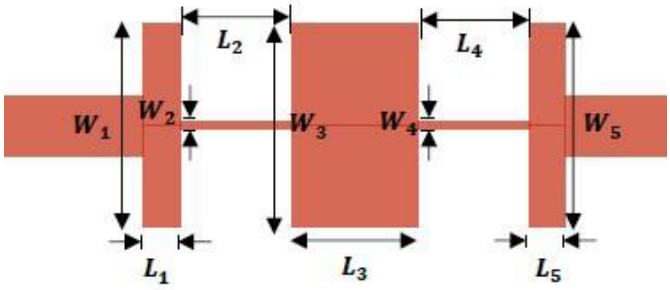

FIGURE 1. The schematic view of the conventional stepped-impedance low-pass filter.

TABLE 1. Dimensions of the conventional stepped-impedance low-pass filter (Unit: mm).

W_1	W_2	W_3	W_4	W_5	W_{total}
11.1	0.4	11.1	0.4	11.1	11.1
L_1	L_2	L_3	L_4	L_5	L_{total}
2	6.2	7	6.2	2	23.4

ventional stepped-impedance low-pass filter can be acquired through the filter design method proposed by Pozar [14]. It can be seen that the conventional stepped-impedance low-pass filter has an order of $N = 5$, and the filter is symmetric where the first step is the same as the fifth step, and the second step is the same as the fourth step. The dimensions of the conventional stepped-impedance low-pass filter are listed in Table 1. As can be seen from Table 1, the overall dimension of the conventional stepped-impedance low-pass filter is 11.1 mm $\times$ 23.4 mm, which is pretty large. To capture the frequency responses of the reflection and transmission coefficients of the conventional stepped-impedance low-pass filter, the conventional stepped-impedance low-pass filter shown in Fig. 1 along with the dimensions listed in Table 1 is simulated with advanced design system (ADS). To verify the simulation result, the conventional stepped-impedance low-pass filter shown in Fig. 1 is implemented as shown in Fig. 2. The real circuit of the conventional stepped-impedance low-pass filter shown in Fig. 2 is then measured with Agilent E5071C using the Keysight 85521A SOLT calibration kit. The measured and simulated frequency responses of the reflection and transmission coefficients are shown in Fig. 3. As can be seen from Fig. 3, the simulation result agrees well with the measurement one. Besides, the -3-dB cutoff frequency is 2.5 GHz, and the attenuation is below -20 dB after 5 GHz, meeting the specification.

3. COMPACT STEPPED-IMPEDANCE LOW-PASS FILTER USING THE COPLANAR OPEN-CIRCUITED STUBS

As the overall dimension of the conventional stepped-impedance low-pass filter listed in Table 1 is pretty large, we will reduce the filter dimension without degrading the filter performance in the following sections. As can be seen from Fig. 1, since the structure of the conventional

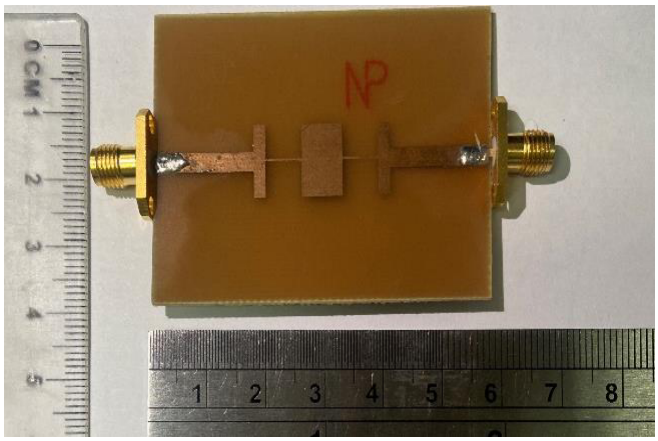

FIGURE 2. The real circuit of the conventional stepped-impedance low-pass filter.

stepped-impedance low-pass filter is symmetric, it is sufficient to miniaturize the first, second, and third steps of the conventional stepped-impedance low-pass filter.

3.1. Miniaturization of First Step

The first step of the conventional stepped-impedance low-pass filter is redrawn in Fig. 4(a), which can be represented by an ideal transmission line having a characteristic impedance of Z_1 and an electrical length of θ_1. The ideal transmission line model shown in Fig. 4(a) is equivalent to a short section of transmission line in series with a capacitor C_1 as shown in Fig. 4(b). The short section of the transmission line has a characteristic impedance of Z_1' and an electrical length of θ_1'. The short section of the transmission line can be implemented with a short section of microstrip line, and the capacitor C_1 can be implemented with two coplanar open-circuited stubs as shown in Fig. 4(c).

As the first step shown in Fig. 4(a) has a length of $L_1 = 2$ mm and a width of $W_1 = 11.1$ mm, the characteristic impedance Z_1 and electrical length θ_1 are calculated as 20 Ω and 14.15° at 2.5 GHz, respectively, by using LinCalc. By equating the *ABCD*-matrix of the ideal transmission line model shown in Fig. 4(a) with the *ABCD*-matrix of the equivalent model shown in Fig. 4(b), the values of the characteristic impedance Z_1' and electrical length θ_1' for the short section of transmission line can be calculated to be 34.4 Ω and 2.8°, respectively, at 2.5 GHz. The value of the capacitance C_1 can be obtained as 0.604 pF at 2.5 GHz. The characteristic impedance $Z_1' = 34.4\,\Omega$ and electrical length $\theta_1' = 2.8°$ for the short section of the transmission line can then be implemented with the microstrip line shown in Fig. 4(c) where the length is $L_1' = 1$ mm, and the width is $W_1' = 5.6$ mm. The capacitance $C_1 = 0.604$ pF can then be implemented with two coplanar open-circuited stubs where each stub has a width of $W_{stub} = 0.6$ mm, a length of $L_{stub} = 2.7$ mm, and a gap of $g = 0.1$ mm, with an impedance of 50 Ω [15].

To verify the equivalence between the ideal transmission line model shown in Fig. 4(a) and the layout shown in Fig. 4(c), the ideal transmission line model shown in Fig. 4(a) and the lay-

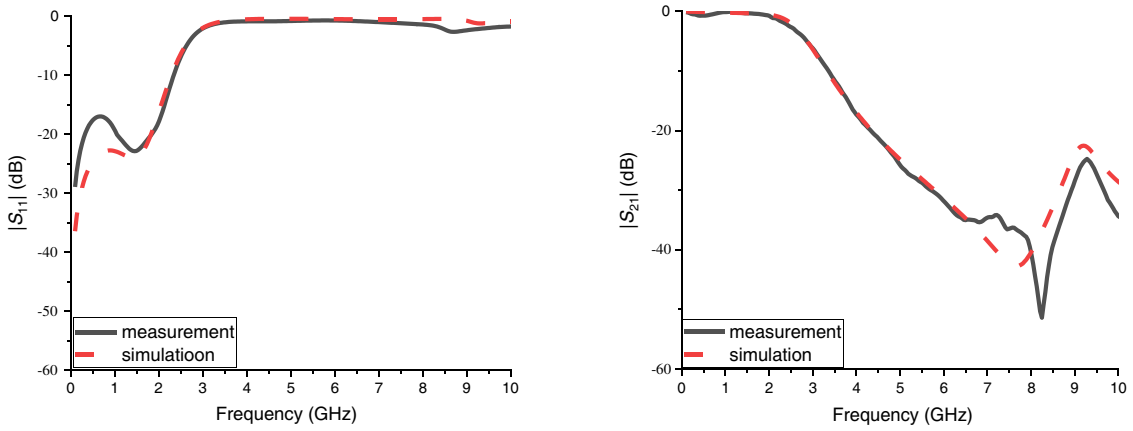

FIGURE 3. Comparison between the simulated and measured frequency responses of the reflection and transmission coefficients for the conventional stepped-impedance low-pass filter. (a) Reflection coefficient. (b) Transmission coefficient.

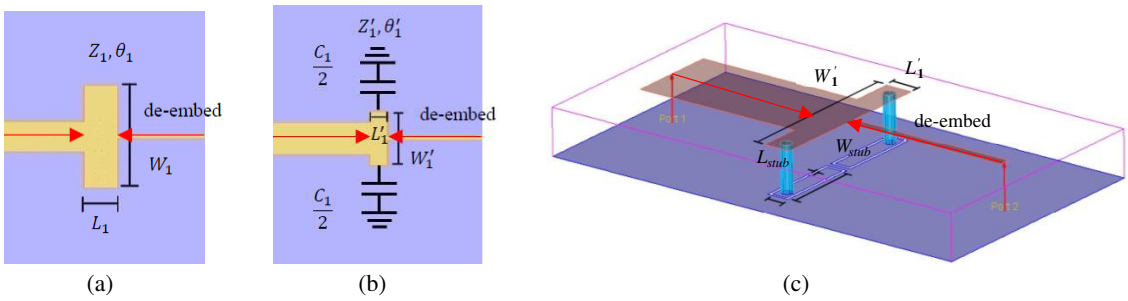

FIGURE 4. The first step of the conventional stepped-impedance low-pass filter. (a) Ideal transmission line model. (b) Equivalent model. (c) Miniaturized layout.

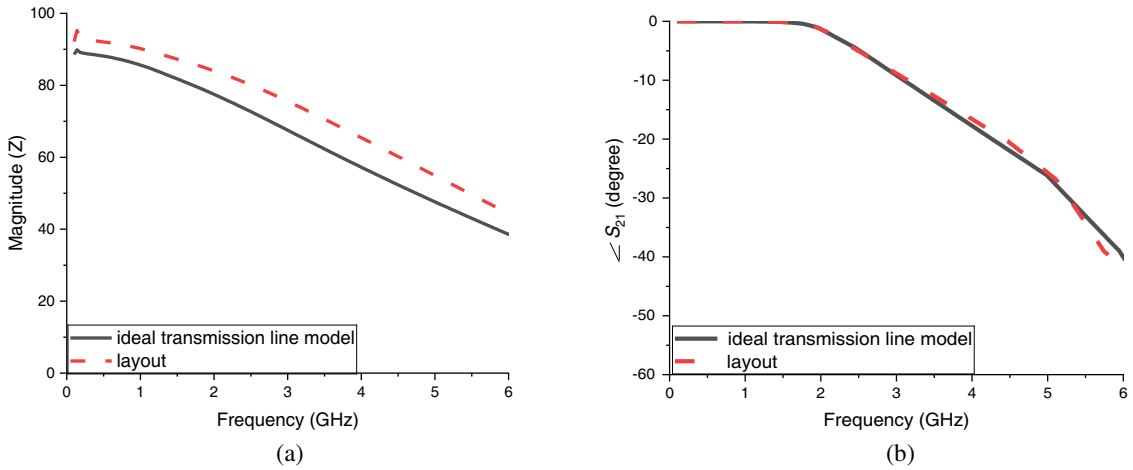

FIGURE 5. Comparison between the frequency responses of the ideal transmission line model and layout. (a) Characteristic impedance. (b) Electrical length.

out shown in Fig. 4(c) are simulated and de-embedded with ADS. The simulated S-parameters are then used to extract these two structures' characteristic impedances and electrical lengths [16]. Fig. 5(a) displays the frequency responses of the characteristic impedances of these two structures while Fig. 5(b) displays the frequency responses of the electrical lengths of these two structures. As can be seen from Fig. 5, the simulated characteristic impedances and electrical lengths of these two structures agree well, showing that the layout in Fig. 4(c) can well represent the ideal transmission line model in Fig. 4(a).

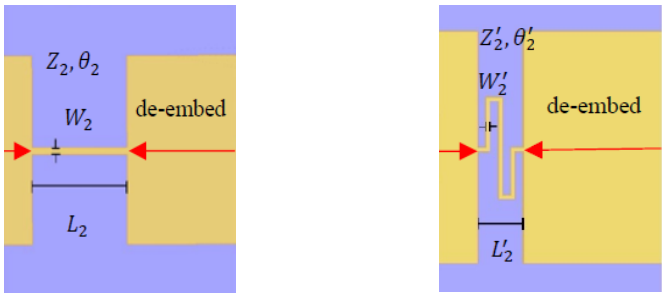

(a) (b)

FIGURE 6. The second step of the conventional stepped-impedance low-pass filter. (a) Thin strip. (b) Meandered line.

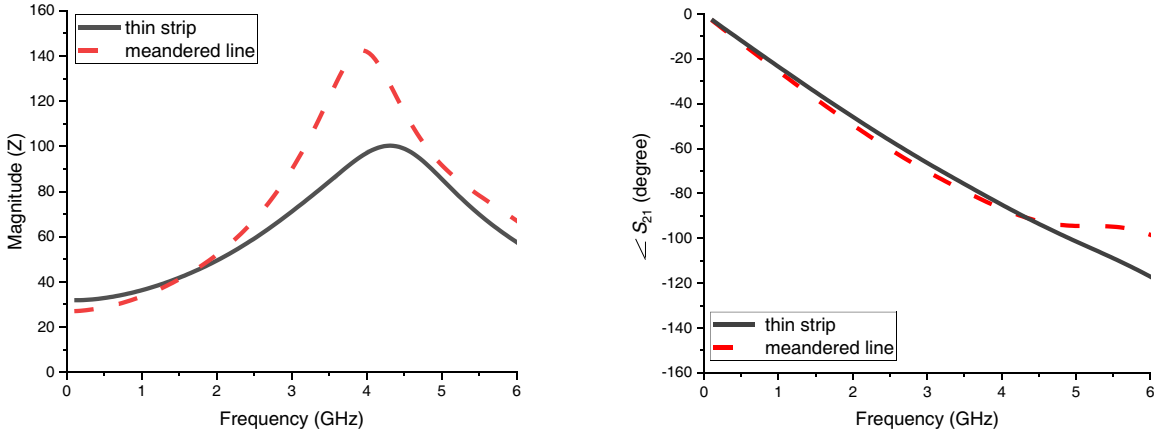

(a) (b)

FIGURE 7. Comparison between the frequency responses of the thin strip and meandered line. (a) Characteristic impedance. (b) Electrical length.

3.2. Miniaturization of Second Step

The second step of the conventional stepped-impedance low-pass filter shown in Fig. 1 is redrawn in Fig. 6(a) for clarity, which has a length of $L_2 = 6.2\,\text{mm}$ and a width of $W_2 = 0.4\,\text{mm}$. As the second step of the conventional stepped-impedance low-pass filter is a thin strip, it is miniaturized through meandering the thin strip as shown in Fig. 6(b) with a spacing of 0.4 mm between the meandered lines. As the meandered lines are close to each other, the coupling between the meandered lines will give rise to the increment of the capacitance between the meandered lines. To compensate for the capacitive increment of the meandered line, the width of the thin strip should be reduced from 0.4 mm to 0.2 mm.

To verify the equivalence between the thin strip shown in Fig. 6(a) and the meandered line shown in Fig. 6(b), the thin strip shown in Fig. 6(a) and the meandered line shown in Fig. 6(b) are simulated with ADS. The simulated S-parameters are then used to extract these two structures' characteristic impedances and electrical lengths. Fig. 7(a) displays the frequency responses of the characteristic impedances of these two structures while Fig. 7(b) displays the frequency responses of the electrical lengths of these two structures. As can be seen from Fig. 7, the simulated characteristic impedances and electrical lengths of these two structures agree well. Even though there is a discrepancy in the simulated characteristic impedances between 3 GHz and 5 GHz, this will not affect the filter's passband performance as this discrepancy is outside the passband 0 GHz to 2 GHz of the low-pass filter. As a result, the meandered line in Fig. 6(b) can well represent the thin strip in Fig. 6(a).

3.3. Miniaturization of Third Step

The third step of the conventional stepped-impedance low-pass filter is redrawn in Fig. 8(a), which can be represented by an ideal transmission line having a characteristic impedance of Z_3 and an electrical length of θ_3. The ideal transmission line model shown in Fig. 8(a) is equivalent to a short section of transmission line in series with a capacitor C_3 as shown in Fig. 8(b). The short section of the transmission line has a characteristic impedance of Z_3' and an electrical length of θ_3'. The short section of the transmission line can be implemented with a short section of the microstrip line, and the capacitor C_3 can be implemented with six coplanar open-circuited stubs as shown in Fig. 8(c).

As the third step has a length of $L_3 = 7\,\text{mm}$ and a width of $W_1 = 11.1\,\text{mm}$, the characteristic impedance Z_3 and electrical length θ_3 are calculated as $20\,\Omega$ and 45.64° at 2.5 GHz, respectively, by using LinCalc. By equating the *ABCD*-matrix of the ideal transmission line model shown in Fig. 8(a) with the *ABCD*-matrix of the equivalent model shown in Fig. 8(b), the

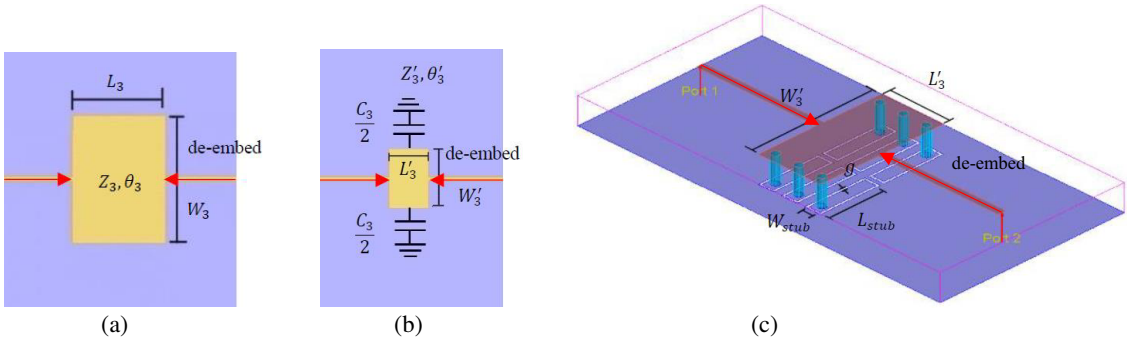

(a) (b) (c)

FIGURE 8. The third step of the conventional stepped-impedance low-pass filter. (a) Ideal transmission line model. (b) Equivalent model. (c) Miniaturized layout.

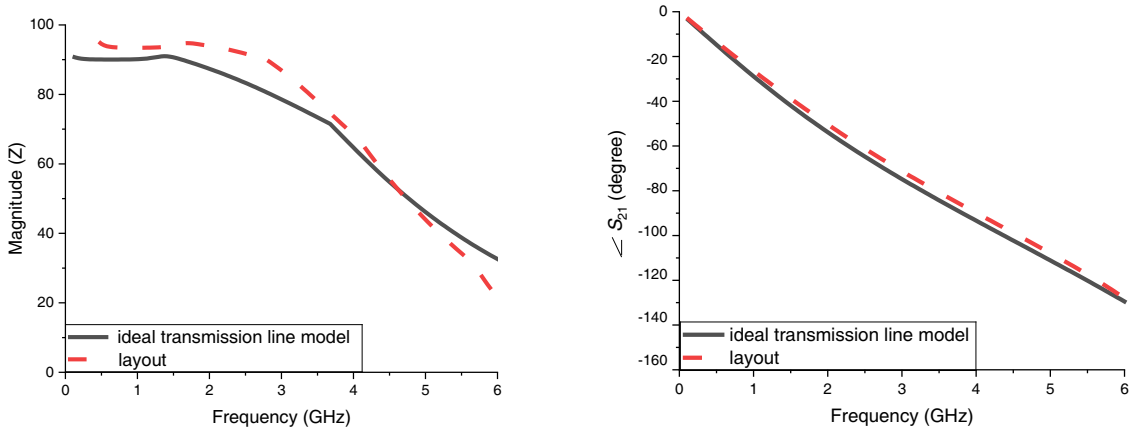

(a) (b)

FIGURE 9. Comparison between the frequency responses of the ideal transmission line model and layout. (a) Characteristic impedance. (b) Electrical length.

values of the characteristic impedance Z_3' and electrical length θ_3' for the short section of transmission line can be calculated to be 30 Ω and 17.94°, respectively, at 2.5 GHz. The value of the capacitance C_3 can be obtained as 1.824 pF at 2.5 GHz. The characteristic impedance $Z_3' = 30\,\Omega$ and electrical length $\theta_3' = 17.94°$ for the short section of the transmission line can then be implemented with the microstrip line shown in Fig. 8(c) where the length is $L_3' = 3$ mm, and the width is $W_3' = 5.6$ mm. The capacitance $C_3 = 1.824$ pF can now be implemented with six coplanar open-circuited stubs where each stub has a width of $W_{stub} = 0.6$ mm, a length of $L_{stub} = 2.4$ mm, and a gap of $g = 0.1$ mm, with an impedance of 50 Ω.

To verify the equivalence between the ideal transmission line model shown in Fig. 8(a) and the layout shown in Fig. 8(c), the ideal transmission line model shown in Fig. 8(a) and the layout shown in Fig. 8(c) are simulated with ADS. The simulated S-parameters are then used to extract these two structures' characteristic impedances and electrical lengths. Fig. 9(a) displays the frequency responses of the characteristic impedances of these two structures while Fig. 9(b) displays the frequency responses of the electrical lengths of these two structures. As can be seen from Fig. 9, the simulated characteristic impedances and electrical lengths of these two structures agree well, showing that the layout in Fig. 8(c) can represent the ideal transmission line model in Fig. 8(a).

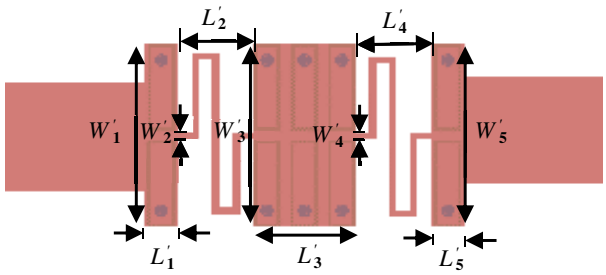

FIGURE 10. The schematic view of the compact stepped-impedance low-pass filter using the coplanar open-circuited stubs.

3.4. Full Filter Structure

By replacing the five steps of the conventional stepped-impedance low-pass filter with the miniaturized steps shown in Fig. 4(c), Fig. 6(b), and Fig. 8(c), the compact stepped-impedance low-pass filter using coplanar open-circuited stubs can be formed as shown in Fig. 10. The dimensions of the compact stepped-impedance low-pass filter using the coplanar open-circuited stubs are listed in Table 2. Comparing the dimensions of the conventional stepped-impedance low-pass filter in Table 1 and the dimensions of the compact stepped-impedance low-pass filter using coplanar open-circuited stubs in Table 2, both the lengths and widths of each section are substantially reduced. As can be seen from Table 2, the overall

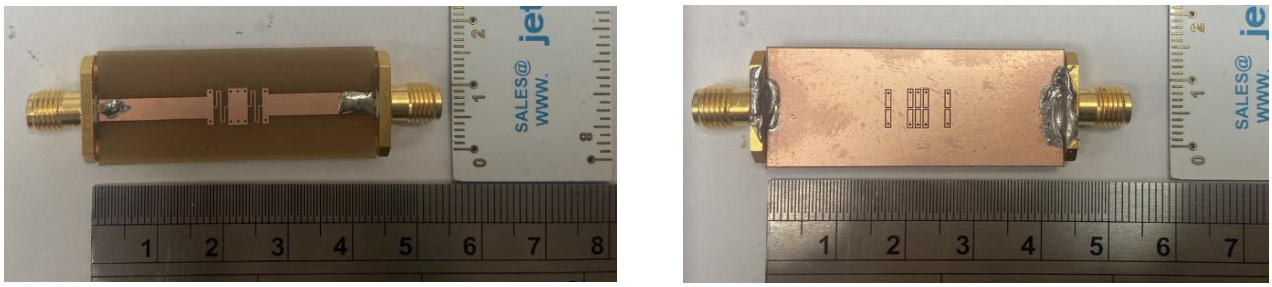

(a) (b)

FIGURE 11. The real circuit of the compact stepped-impedance low-pass filter using the coplanar open-circuited stubs. (a) Top view. (b) Bottom view.

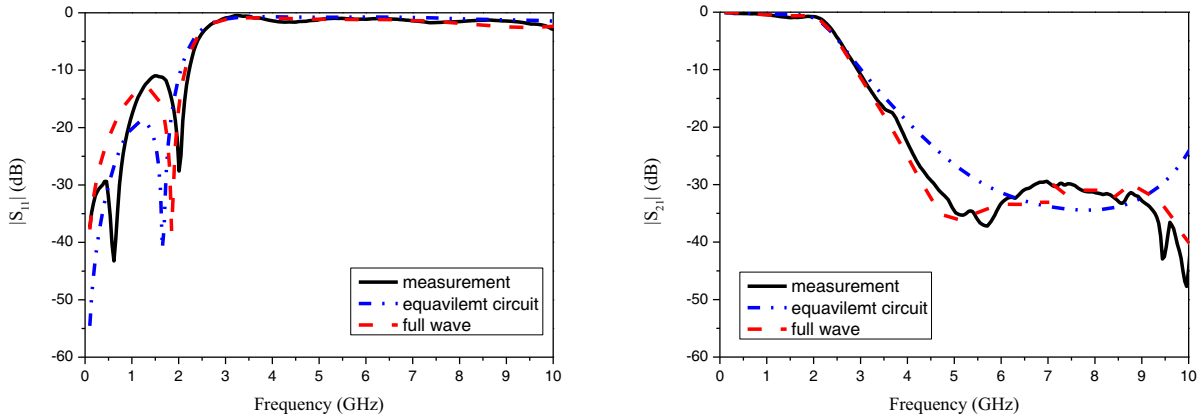

(a) (b)

FIGURE 12. Comparison between the simulated and measured frequency responses of the reflection and transmission coefficients for the compact stepped-impedance low-pass filter using the coplanar open-circuited stubs. (a) Reflection coefficient. (b) Transmission coefficient.

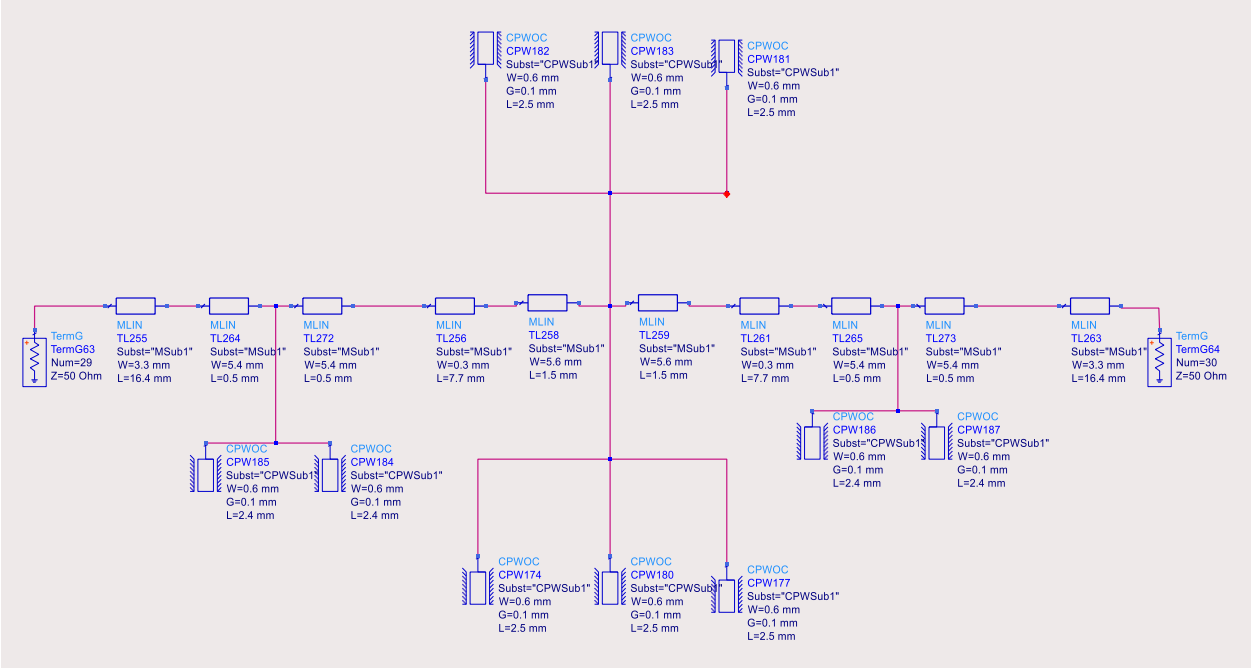

FIGURE 13. The equivalent circuit of the compact stepped-impedance low-pass filter using the coplanar open-circuited stubs.

TABLE 2. Dimensions of the compact stepped-impedance low-pass filter using the coplanar open-circuited stubs (Unit: mm).

W'_1	W'_2	W'_3	W'_4	W'_5	W'_{total}
5.6	0.2	5.6	0.2	5.6	5.6
L'_1	L'_2	L'_3	L'_4	L'_5	L'_{total}
1	2.2	3	2.2	1	9.4

TABLE 3. Comparison between the conventional stepped-impedance low-pass filter and the compact stepped-impedance low-pass filter using the coplanar open-circuited stubs.

	Dimension	−3-dB Cutoff Frequency	Attenuation
Conventional Filter	11.1 mm × 23.4 mm	2.5	−20 dB
Compact Filter	5.6 mm × 9.4 mm	2.5	−30 dB

dimension of the compact stepped-impedance low-pass filter using the coplanar open-circuited stubs is 5.6 mm × 9.4 mm, which is much smaller than the dimension of the conventional stepped-impedance low-pass filter (11.1 mm × 23.4 mm), amounting to 79.83% reduction.

To capture the frequency responses of the reflection and transmission coefficients of the compact stepped-impedance low-pass filter using the coplanar open-circuited stubs, the compact stepped-impedance low-pass filter using coplanar open-circuited stubs shown in Fig. 10 along with the dimensions listed in Table 2 is simulated with ADS. To verify the simulation result, the compact stepped-impedance low-pass filter using coplanar open-circuited stubs shown in Fig. 10 is implemented as shown in Fig. 11. The real circuit of the compact stepped-impedance low-pass filter using coplanar open-circuited stubs shown in Fig. 11 is then measured with Agilent E5071C using the Keysight 85521A SOLT calibration kit. The measured and simulated frequency responses of the reflection and transmission coefficients are shown in Fig. 12. As can be seen from Fig. 12, the simulation result agrees well with the measurement one. The −3-dB cutoff frequency is 2.5 GHz, and the attenuation is below −30 dB after 5 GHz, which is less than −20 dB of the conventional stepped-impedance low-pass filter, meeting the specifications of the required low-pass filter. To verify the effectiveness of the equivalent circuit, the equivalent circuit of the compact stepped-impedance low-pass filter using the coplanar open-circuited stubs is demonstrated in Fig. 13. The equivalent circuit of the compact stepped-impedance low-pass filter using the coplanar open-circuited stubs shown in Fig. 13 is simulated with ADS, and the frequency responses of the reflection and transmission coefficients are also shown in Fig. 12. As can be seen from Fig. 12, the simulation results also agree well with the full wave and measurement results.

4. CONCLUSION

This paper proposes a compact stepped-impedance low-pass filter using coplanar open-circuited stubs. As the coplanar open-circuited stubs are implemented underneath the stepped-impedance low-pass filter, the size of the stepped-impedance low-pass filter can be significantly reduced. The overall dimension of the compact stepped-impedance low-pass filter using the coplanar open-circuited stubs is 5.6 mm × 9.4 mm, which is much smaller than the dimension of the conventional stepped-impedance low-pass filter (11.1 mm × 23.4 mm), amounting to 79.83% reduction. In addition, the −3-dB cutoff frequency is 2.5 GHz, and the attenuation is below −30 dB, which is less than −20 dB of the conventional stepped-impedance low-pass filter. The comparison between the conventional stepped-impedance low pass filter and the compact stepped-impedance low-pass filter using coplanar open-circuited stubs is summarized in Table 3. To verify the simulation result, the conventional stepped-impedance low-pass filter and the compact stepped-impedance low-pass filter using coplanar open-circuited stubs are fabricated and measured where the measurement results agree well with the simulation ones.

ACKNOWLEDGEMENT

This work was supported in part by the National Science and Technology Council, Taiwan, under Grant NSTC 114-2221-E-011-075. The authors would like to thank Wireless Communications & Applied Electromagnetic Laboratory, National Taiwan University of Science and Technology, Taipei, Taiwan, for providing the simulation environment. Also, they thank Prof. C.-H. Tseng, National Taiwan University of Science and Technology, for providing the measurement instruments.

REFERENCES

[1] Cohn, S. B., "Parallel-coupled transmission-line-resonator filters," *IRE Transactions on Microwave Theory and Techniques*, Vol. 6, No. 2, 223–231, Apr. 1958.

[2] Makimoto, M. and S. Yamashita, "Bandpass filters using parallel coupled stripline stepped impedance resonators," *IEEE Transactions on Microwave Theory and Techniques*, Vol. 28, No. 12, 1413–1417, 1980.

[3] Tang, C.-W. and M.-G. Chen, "Wide stopband parallel-coupled stacked SIRs bandpass filters with open-stub lines," *IEEE Microwave and Wireless Components Letters*, Vol. 16, No. 12, 666–

668, Dec. 2006.

[4] Tang, C.-W. and Y.-K. Hsu, "Design of a wide stopband microstrip bandpass filter with asymmetric resonators," *IEEE Microwave and Wireless Components Letters*, Vol. 18, No. 2, 91–93, Feb. 2008.

[5] Tang, C.-W. and Y.-K. Hsu, "A microstrip bandpass filter with ultra-wide stopband," *IEEE Transactions on Microwave Theory and Techniques*, Vol. 56, No. 6, 1468–1472, Jun. 2008.

[6] Mandal, M. K. and S. Sanyal, "A novel defected ground structure for planar circuits," *IEEE Microwave and Wireless Components Letters*, Vol. 16, No. 2, 93–95, 2006.

[7] El-Halabi, H., S. Abou-Chahine, D. Kaddour, E. Pistono, and P. Ferrari, "DGS-SMS compact fifth order low pass filter," in *2017 International Conference on High Performance Computing & Simulation (HPCS)*, 274–277, Genoa, Italy, Jul. 2017.

[8] Ahn, D., J.-S. Park, C.-S. Kim, J. Kim, Y. Qian, and T. Itoh, "A design of the low-pass filter using the novel microstrip defected ground structure," *IEEE Transactions on Microwave Theory and Techniques*, Vol. 49, No. 1, 86–93, 2001.

[9] Boudaa, S., M. Challal, R. Mehani, and D. Rabahallah, "Miniaturized ultra-wide stopband microstrip low pass filter design," in *2015 4th International Conference on Electrical Engineering (ICEE)*, 1–3, Boumerdes, Algeria, Dec. 2015.

[10] Luo, S., L. Zhu, and S. Sun, "Stopband-expanded low-pass filters using microstrip coupled-line hairpin units," *IEEE Microwave and Wireless Components Letters*, Vol. 18, No. 8, 506–508, 2008.

[11] Hsieh, L.-H. and K. Chang, "Compact elliptic-function low-pass filters using microstrip stepped-impedance hairpin resonators," *IEEE Transactions on Microwave Theory and Techniques*, Vol. 51, No. 1, 193–199, 2003.

[12] Zhang, F., S. Liu, P. Zhao, M. Du, X. Zhang, and J. Xu, "Compact ultra-wide stopband lowpass filter using transformed stepped impedance hairpin resonator," in *2017 IEEE International Symposium on Antennas and Propagation & USNC/URSI National Radio Science Meeting*, 2227–2228, San Diego, CA, USA, Jul. 2017.

[13] Dahlan, S. H. and M. Esa, "Miniaturized low pass filter using modified unifolded single hairpin-line resonator for microwave communication systems," in *2006 International RF and Microwave Conference*, 16–20, Putra Jaya, Malaysia, Sep. 2006.

[14] Pozar, D. M., *Microwave Engineering*, 3rd ed., John Wiley & Sons, 2005.

[15] Matthaei, G. L., L. Young, and E. M. T. Jones, *Microwave Filters, Impedance-Matching Networks, and Coupling Structures*, Artech House, 1980.

[16] Yan, Z.-S., "Reduction of common-mode and differential-mode noises for multilayers differential transmission line," Master's degree thesis, National Taiwan University of Science and Technology, Taipei City, Taiwan, 2016.